



## Partial discharge detection by using combined VHF and AE sensors in XLPE power cables

Ahmad Moradi<sup>1\*</sup>, Seyyed Mohammad Hassan Hosseini<sup>1</sup>

<sup>1</sup> Department of Electrical Engineering, South Tehran Branch, Islamic Azad University, Tehran, Iran.

Received: 21-Feb-2019, Revised: 07-July-2019, Accepted: 09-July-2019.

### Abstract

The purpose of this article is troubleshooting and detection of a partial discharge in cross-linked polyethylene (XLPE) cable by combining two very-high-frequency (VHF) and acoustic emission (AE) sensors, which is a novel approach to troubleshooting. The small size of these signals is the main problem in partial discharge (PD) measurements, which might cause the signal being mixed with noise completely and make troubleshooting difficult to get. Hence, attention has been paid to high bandwidth to eliminate disturbing noise. In this paper, Rogowski's coil is designed as a kind of VHF sensor to address the problems in this regard. Then, it simulates and examines the characteristics of the partial discharge in the power cables that have been occurred due to the existence of a cavity. In the end, in order to prove the efficiency of the intended method, the actual partial discharge test was performed using the VHF and AE sensors. The combination of two VHF and AE sensors is capable of eliminating electrical interference and electromagnetic noise in the test site, as well as identifying different types of discharge, and providing a model for troubleshooting partial discharges in online and offline tests. In addition, due to the simple design and installation of the sensor in the equipment and not being mandatory to cut off equipment from the network, employing this method can be highly economical.

**Keywords:** PD, VHF, AE, XLPE, cable, capacitive model, Rogowski coil.

### 1. INTRODUCTION

Partial discharges in power cables usually occur due to the presence of holes, cracks, contaminants, and improper installation

(human error) [1]. Since the failure of partial discharge in the cable insulation may result in complete failure of the insulation, and consequently the failure of the power grid,

---

\*Corresponding Author's Email:  
st\_a.moradi@azad.ac.ir

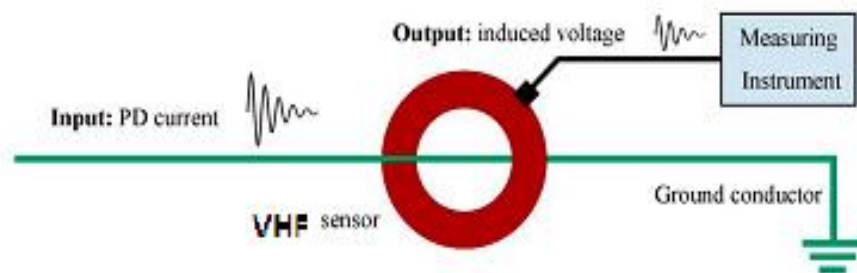


*Fig. 1. Schematic view of the location of the VHF sensor.*

timely detection and troubleshooting the equipment have become an important issue in the grid. Troubleshooting is done in different forms online, on-site and offline. Offline procedures require separating the desired part of the circuit and interrupting the load, this method is often time-consuming and costly because of the separation of equipment from the network [2-3].

Online and on-site shortcomings require the recording and use of data received by their own sensors over a period of time in order to provide an appropriate pattern for detecting defects [4]. Also, in the online and on-site detections, changes to the setting of the high voltage equipment or the equipment themselves were usually made, which is not acceptable in the power system.

Troubleshooting accuracy usually depends on the following:

1. The method used to troubleshoot
2. Repetition rate and monitoring time
3. The sensor performance diagnostics

Continuous monitoring involves steps:  
 A) Receive information and data from monitored equipment by the defective sensor,  
 B) sending these data to the processing system, C) Processing information by the

processing unit and determining the appropriate model for troubleshooting [5-6].

Due to the low frequency of partial discharge and fast transient mode, it is not possible to protect the system against this error in the normal way. Therefore, to monitor the system against this type of error, the use of high-frequency sensors is essential. The choice of sensor type depends on the noise bandwidth and the investigated quantity (voltage, current, and load). It is possible to use inductive sensors at frequencies below 100 MHz and capacitive sensors for up to 300 MHz [7]. In addition, the combination of sensors gives us the ability to cover a larger range for troubleshooting. High-frequency sensors usually sample the current signal, and these types of sensors are CT-like.

The purpose of this article is to use the Rogowski coil as a frequency current transformer. This transformer measures the flow of the zero sequence of the cable and reveals a partial discharge voltage with signal changes. Another advantage of this coil is the lack of saturation at high frequencies. The sensor output signal is amplified due to its small size by an analog booster with a gain of over 100. Fig. 1 shows the Rogowski coil

location as the VHF sensor in the power cable.

A Rogowski coil with a ferromagnetic core operating in the range of 1 to 60 MHz has been used as a type of VHF sensor and able to detect three different types of partial discharge in high voltage 110 kV cables, detecting and reduce a large amount of environmental noise [8]. Rogowski's coil can be used as a VHF sensor to monitor high-pressure cables and joints to troubleshoot a variety of partial discharge, and can be safely and easily installed in equipment without changing the structure of the equipment [9]. This type of troubleshooting has been able to eliminate noise widely [10]. In the use of the VHF sensor and capacitor coupler simultaneously, we can detect the shortcomings of cable and other equipment at short distances and also detect partial discharge of fewer than 3 PCs, It can also be done both online and offline [11].

An acoustic method is also used to locate the fault location and identify the type of discharge. These signals are generated by partial discharge at defective points of the insulator and received by an acoustic sensor. The detection of acoustic waves, due to minor evacuation in cables and other high-pressure equipment, has the advantage of non-interference. This method is an easy way to use and suitable for monitoring high-pressure equipment and periodic tests. Another advantage of this approach is to pay attention to the size of the received sound waves due to partial discharge, which makes it possible to detect the location and size of the partial discharges. Furthermore, this method has turned into a reliable way to

troubleshoot a partial discharge in high-pressure devices [12-15].

Combining the results of two VHF and acoustic sensors to troubleshoot two specific types of incomplete electrical evacuations in a high voltage cable, which was the object of research, has been a lot of efficiencies and ability to detect over 90% of these electrical discharges. Moreover, the mentioned combination propounds the correct pattern of this kind of fault and eliminates excessive noise as well as identifying the location of the defect, according to the signals received by the acoustic sensor [16]. Therefore, this method is suitable for detecting on-site minor discharges on cable accessories and HV XLPE cables. This research and other previous studies have shown that detection of on-site discharge in the VHF range with high reliability is possible. In addition, this study will show that this way troubleshooting can detect Partial discharge (PD), Corona discharge, and floating discharge simultaneously and defect locating. likewise, electrical and electromagnetic noise is largely taken away.

## **2. MODELING AND SIMULATION**

### **2.1. Designing a VHF Sensor and Related Results**

This type of coil can be used instead of the VHF sensor. Due to the low cost of making this type of coil and the need to change the structure of our system, we decided to design and manufacture it[17]. The Rogowski-coil current transformer structure (VHF sensor) can be divided into a Rogowski converter, analog signal processing unit, digital signal processing unit, and power supply unit. The

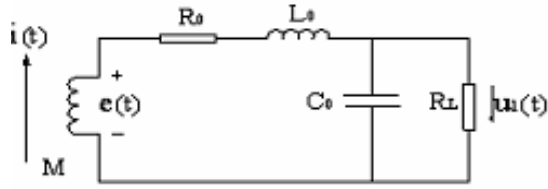
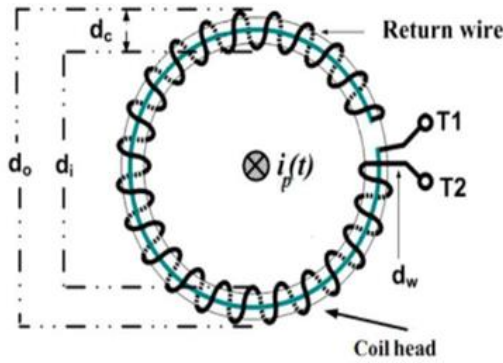


Fig. 2. Equivalent circuit of a Rogowski transducer circuit.



(a)



(b)

Fig. 3. (a) View of Rogowski's coil and its Elements and (b) view of a Rogowski coil with an air core.

equivalent circuit of the Rogowski converter is shown in Fig 2. Rogowski's converter is relatively small due to the use of an air core. The Rogowski- coil current transformer, dedicated to this test, is equipped with a very large load. When the measured current has a low frequency, the internal resistance and internal capacity are small enough to be neglected, and the secondary side of the

Rogowski converter is in the open circuit state [18-21].

At the moment, the output voltage is:

$$U_i(t) \approx e(t) = -M \cdot di/dt \quad (1)$$

The transfer function for Rogowski transducer according to the equivalent circuit is:

$$\begin{aligned} H_i(s) &= \frac{U_i(s)}{I(s)} \\ &= \frac{Ms}{L_o C_o s^2 + \left(\frac{L_o}{R_L} + R_o C_o\right) s + \left(\frac{R_o}{R_L} + 1\right)} \end{aligned} \quad (2)$$

The undamped natural angular frequency:

$$\omega_s = \frac{1}{\sqrt{L_o C_o}} \sqrt{\frac{R_L + R_o}{R_L}} \quad (3)$$

Damping radding is equal to:

$$\zeta = \frac{1}{2\sqrt{L_o C_o}} \left(\frac{L_o}{R_L} + R_o C_o\right) \sqrt{\frac{R_L}{R_L + R_o}} \quad (4)$$

Then the transfer function is:

$$H(s) = \frac{M}{L_o C_o} \cdot \frac{s}{(s - S_1) \cdot (s - S_2)} \quad (5)$$

where characteristic roots are  $S_{1,2} = \zeta \omega_0 \pm \omega_0 \sqrt{(\zeta \times \zeta) - 1}$ ; therefore, the manufacturers determine the number of turns of coil,  $n$ , depending on the desired value of the mutual inductance  $M$ , and the coil induction is  $L_o = M.N$ . Then, the main factors affecting the frequency characteristics of the Rogowski transducer are the internal resistance of the coil and distributed capacitance.

As shown in Fig 3, the wire is wound such that the winding start from the first end, progresses towards the other end and

returning through the center of the coil back to the first end, so that both terminals are at the same end of the coil. Number of turns (N), outer diameter of coil ( $d_o$ ), and inner diameter of coil ( $d_i$ ) are the major physical parameters of coil head (Table 1). Its physical parameters are selected based on the application requirements of the coil.

The overall transfer function of Rogowski-coil Current Transformer is:

$$H(s) = H_1(s)H_2(s)H_3(s) \quad (6)$$

where  $H_1(s)$ ,  $H_2(s)$ ,  $H_3(s)$  are the transfer function of Rogowski transducer respectively, the integral amplification and phase compensation part.

Accordingly, the Rogowski transducer transfer function is an integral amplified function and phase compensation:

$$H_2(s) = \frac{K_2}{1 + RCs} \quad (7)$$

$$H_3(s) = \frac{1 - K_3s}{1 + K_3s} \quad (8)$$

In which the values  $RC=0.066$ ,  $K_2=219.56$  are expressed. Based on the prototype parameters, the transverse Bode diagram is generally shown as shown in Fig4. One can guess that the relative error and phase error of the Rogowski-coil current transformer is between 10-200 Hz. The phase error is higher in the high-frequency range.

## 2.2. Partial Discharge Simulation

The model is used for simulation is shown in Fig 5. The model, used in this paper, is the modified version of the capacitive model. A model that simulates a cavity in a surface cut of the cable length [22]. Where  $C_{scor}$  represents the insulation symbol around the

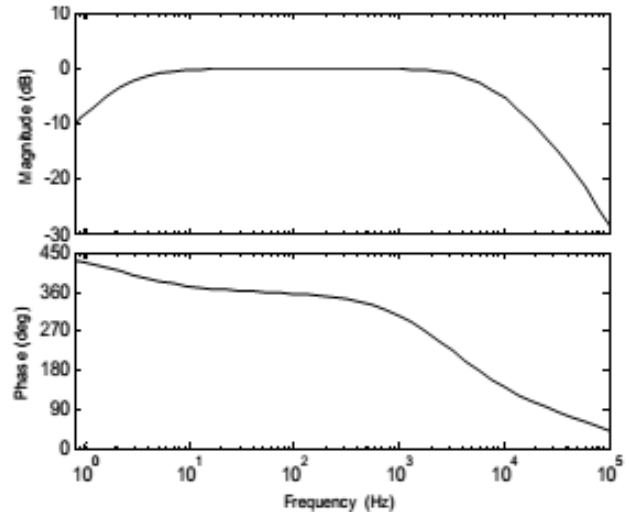


Fig. 4. Bode Transformation by Rogowski

Table 1. Physical Properties of Rogowski coil.

Name of parameters	Symbol	Specification
Number of turns	N	<b>100</b>
Outer diameter of coil	$d_o$	<b>16.1 cm</b>
Inner diameter of coil	$d_i$	<b>14.1 cm</b>
Core diameter	$d_{rc}$	<b>2 cm</b>

cavity and these values are in series with the cavity capacitor in this model. These values are corrected by the correction factor  $K_{(ef)}$  proposed for correction, and  $R_{scor}$  is the corresponding resistance. The corresponding  $C_{void}$  value is the cavity capacitance and  $R_{void}$  is the corresponding resistance value of the cavity.

Breaker once apply for discharge switching voltage 25 kV to 50 Hz becomes clear. Then, using an oscilloscope, the voltage and voltage of the PD and the applied voltage waveform are observed.

The electric model should be able to

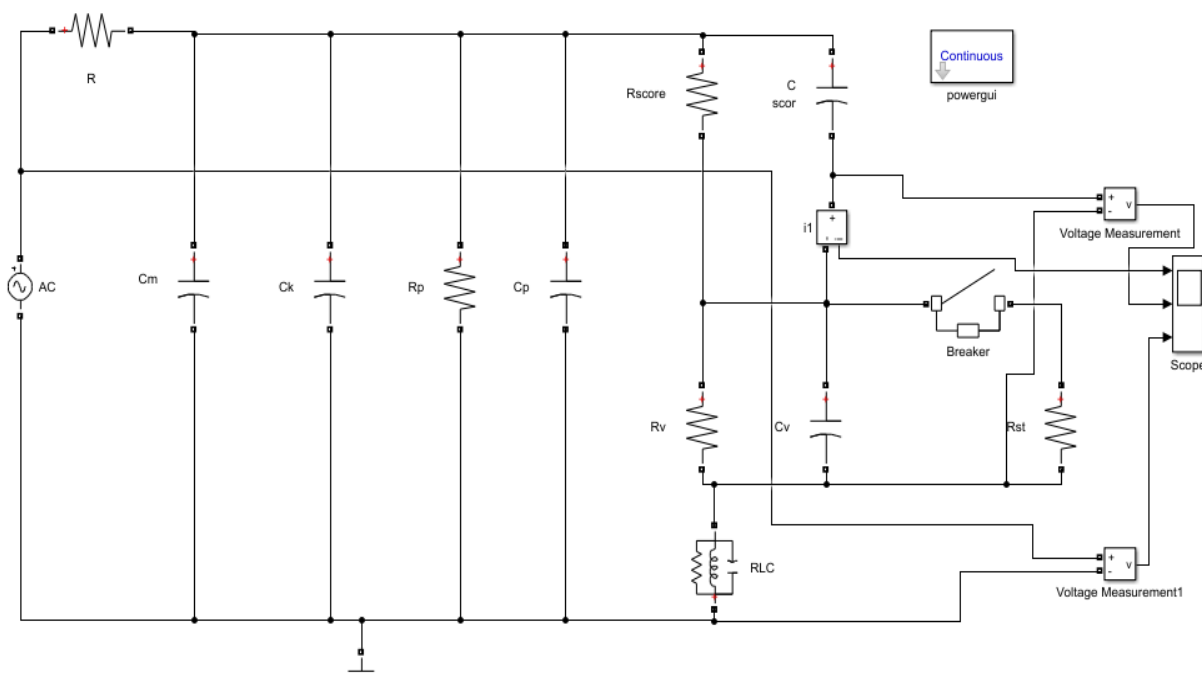


Fig. 5. Equivalent circuit simulated by MATLAB for partial discharge in cable.

Table 2. The values of simulation parameters for different positions of cavity.

Calculated parameters	Void distance from conductor (mm)				
	1.5	2	2.5	3	3.5
$C_P(\text{F})$	$2.69 \times 10^{-10}$	$2.69 \times 10^{-10}$	$2.69 \times 10^{-10}$	$2.69 \times 10^{-10}$	$2.69 \times 10^{-10}$
$R_P(\Omega)$	$1.24 \times 10^{15}$	$1.24 \times 10^{15}$	$1.24 \times 10^{15}$	$1.24 \times 10^{15}$	$1.24 \times 10^{15}$
$C_{\text{scor}}(\text{F})$	$1.045 \times 10^{-14}$	$9.54 \times 10^{-15}$	$8.76 \times 10^{-15}$	$8.11 \times 10^{-15}$	$7.53 \times 10^{-15}$
$R_{\text{scor}}(\Omega)$	$3.2 \times 10^{19}$	$3.51 \times 10^{19}$	$3.82 \times 10^{19}$	$4.13 \times 10^{19}$	$4.44 \times 10^{19}$
$C_{\text{void}}(\text{F})$	$1.86 \times 10^{-14}$	$1.86 \times 10^{-14}$	$1.86 \times 10^{-14}$	$1.86 \times 10^{-14}$	$1.86 \times 10^{-14}$
$R_{\text{void}}(\Omega)$	$1 \times 10^{11}$	$1 \times 10^{11}$	$1 \times 10^{11}$	$1 \times 10^{11}$	$1 \times 10^{11}$
$R_{\text{str}}(\Omega)$	$10 \times 10^3$	$10 \times 10^3$	$10 \times 10^3$	$10 \times 10^3$	$10 \times 10^3$
$C_{\text{str}}(\text{F})$	$1.86 \times 10^{-15}$	$1.86 \times 10^{-15}$	$1.86 \times 10^{-15}$	$1.86 \times 10^{-15}$	$1.86 \times 10^{-15}$

describe the material specifications and partial discharge activities. Various models have been presented to evaluate partial evacuation by many researchers. In this model, a scenario based on real-world testing

is considered to be fully simulated and high-reliability output is considered [23-24]. This is because of the use of the  $C_k$  coupling capacitor, a high voltage measurement capacitor  $C_m$  and a  $R_{v1}$  detector are shown by

a parallel RLC connection, and these items are required for a standard PD case. Here, the values of  $C_m$  and  $C_k$  are expressed as 100pF and 1000F consecutively. In the meanwhile, the detector device values are represented by RLC values  $R=50\Omega$ ,  $L=0.63\text{mH}$ , and  $C=0.47\text{F}$ , respectively. The domain scopes show the applied voltage waveforms, minor discharge voltages, and partial discharge current for comparison with effective values. The

calculations are made for the different void locations within the insulation and the result obtained is given in the tabular form in Table2.

The resulting simulations for the different void locations are shown below. The locations considered are 1.0mm, 1.5mm, 2.0mm, 2.5mm and 3.0mm distances from the conductor.

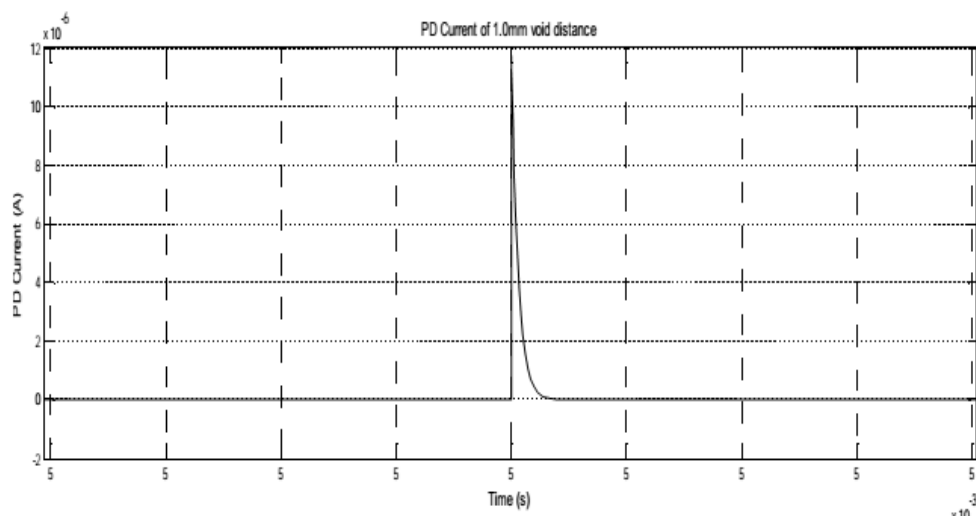


**Fig. 6.** Shows a partial drain flow at a distance of 1.0mm from the cavity.

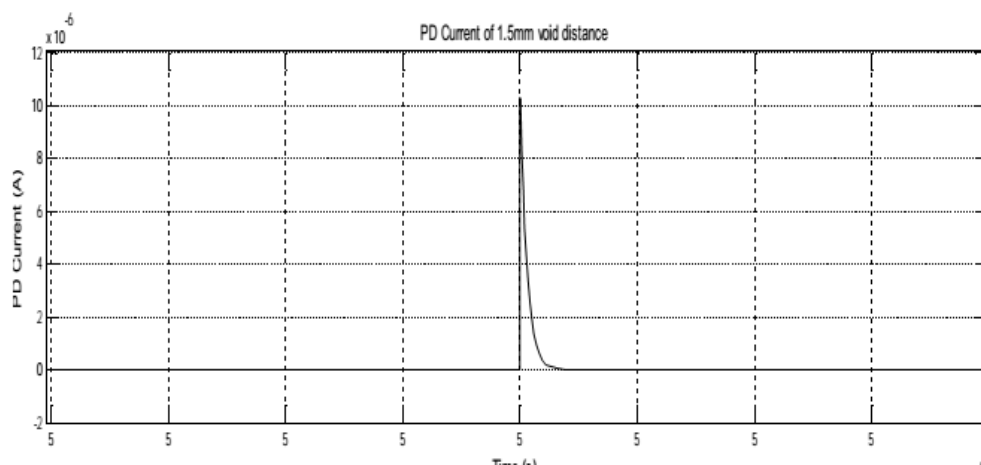


**Fig. 7.** Shows a partial drain flow at a distance of 1.5 mm from the cavity.

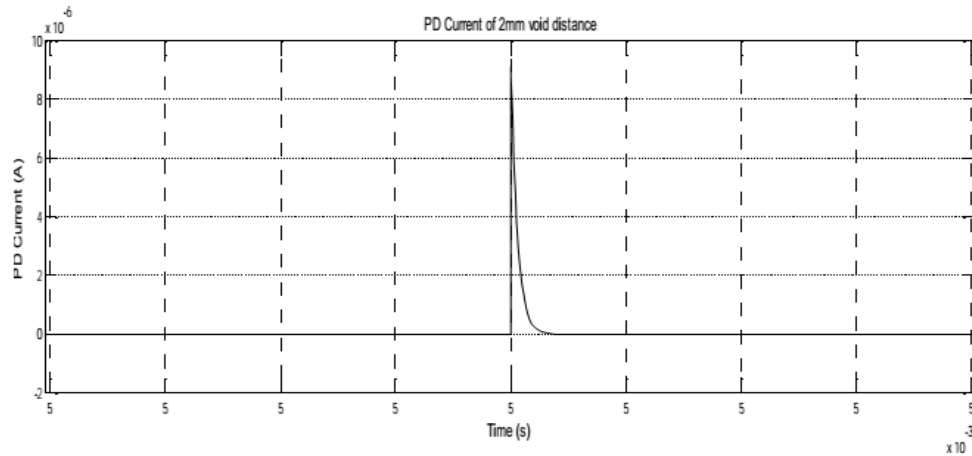


**Fig. 8.** Shows a partial drain flow at a distance of 2.0 mm from the cavity.

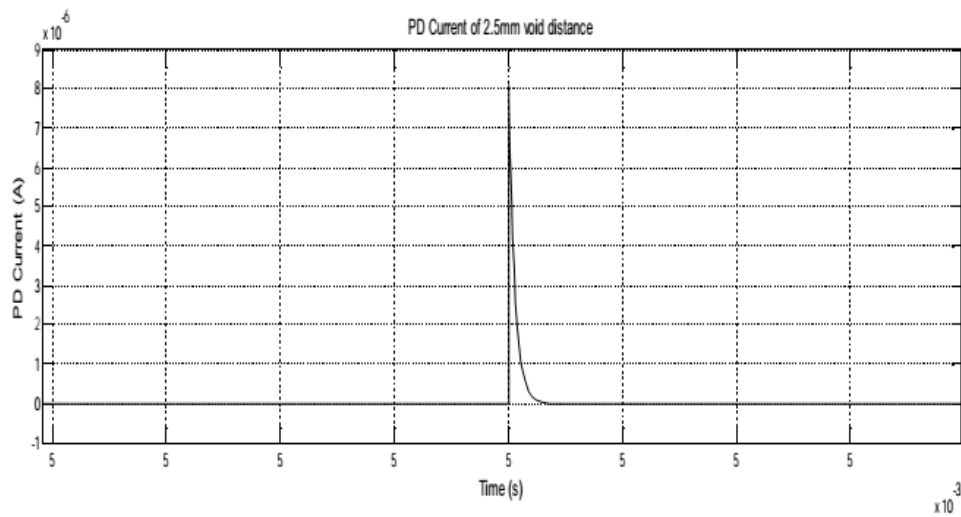


**Fig. 9.** Shows a partial drain flow at a distance of 2.5 mm from the cavity.

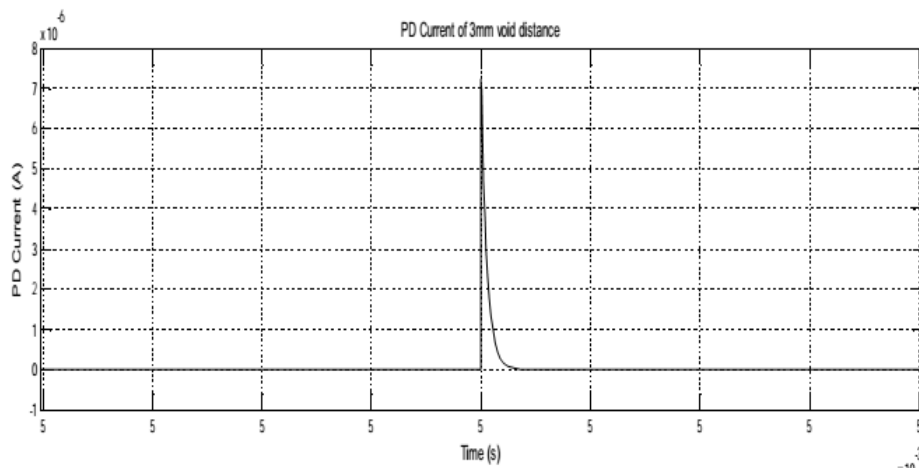


**Fig. 10.** Shows a partial drain flow at a distance of 3.0 mm from the cavity.

**Table 3. Partial drain flows at each interval from the cavity.**

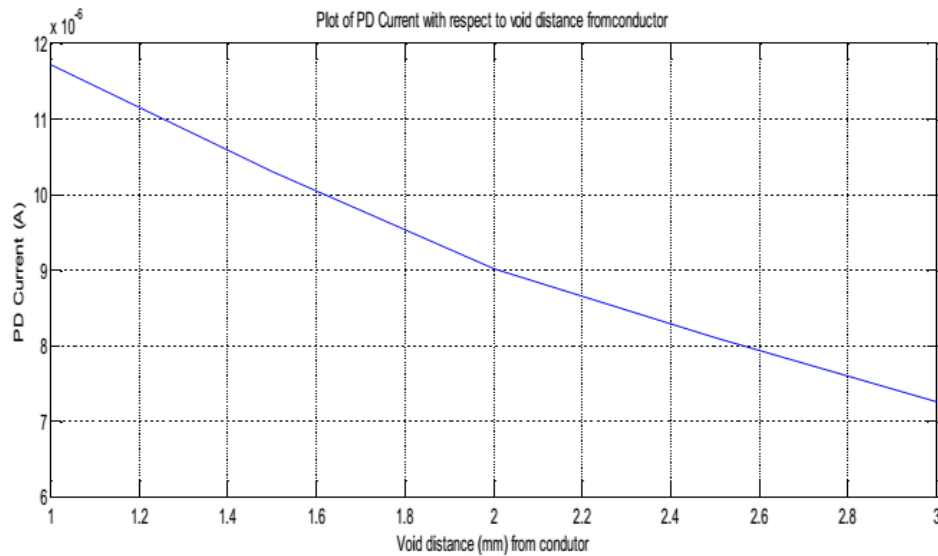
Void distances(mm)	PD current
1	$1.17 \times 10^{-5}$
1.5	$1.03 \times 10^{-5}$
2	$9.01 \times 10^{-6}$
2.5	$8.1 \times 10^{-6}$
3	$7.24 \times 10^{-6}$

The amplitude of each PD current with respect to its void distances from the conductor is given in the tabular form in table 3, and the graph comparison is given in fig 11.

To simulate a portion of the cable, for example, consider that a cavity in which it is intended. The results, such as the function of the phase, are usually used to describe PD behaviors. These results for analyzing PD behaviors should be a function of a phase or a function of time. In order to extract these

results, fundamental quantities should be studied over a period of time greater than the voltage period. Therefore, the results such as the number of discharge pulses in more than half the cycle  $N(t)$  and the alternating voltage changes with time  $U_i(t)$  are used to describe the insulation conditions at the PD occurrences. As shown in Fig 6 through 10, the cavity's flow is obtained for different cavity intervals and locations. As shown in Fig 11, the partial discharge current is even greater as the cavity is closer to the conductor. And Fig 12 shows that the larger the pore size makes the partial discharges current bigger. This indicates the difference in the size of different discharge points during the test process.

We simulate acoustic waves based on the Radiate Basis Function (RBF), The results of figure 13 are then obtained by coding in MATLAB to simulate the acoustic waveform.

**Fig. 11. Flow Chart of partial discharge in terms of distance from the hole.**

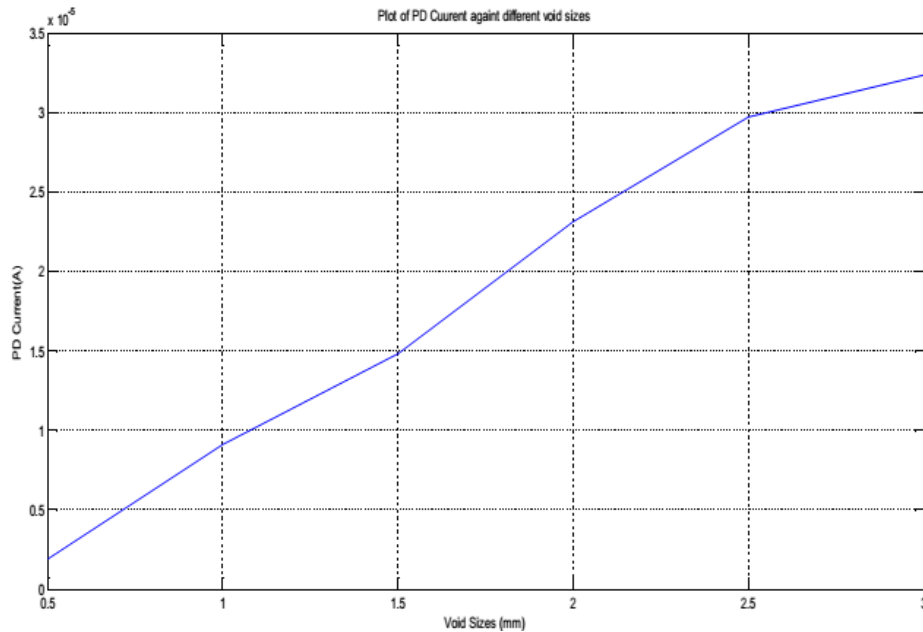


*Fig. 12. Shows a partial discharge diagram in terms of the size of the cavity.*

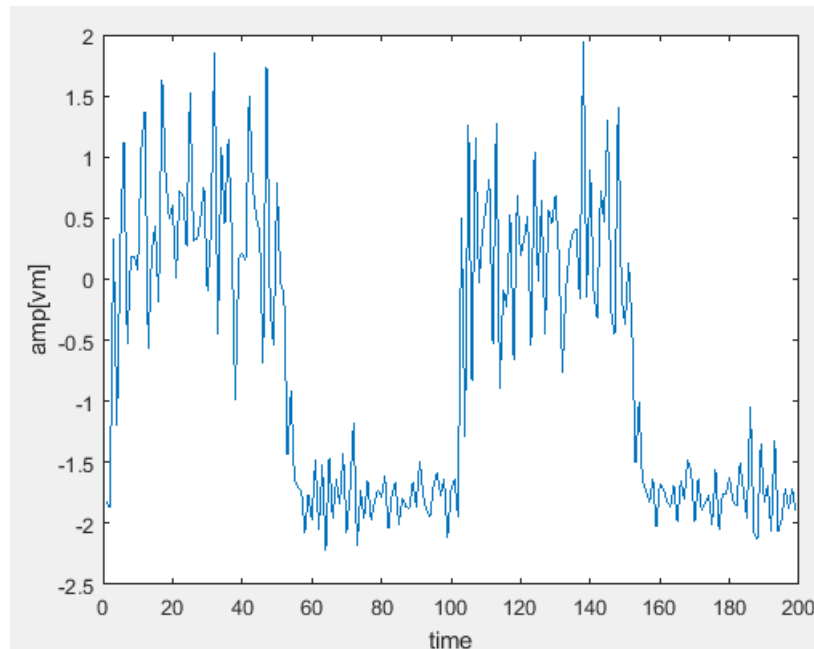


*Fig. 13. Acoustic simulation results*

### 3. EXPERIMENTAL RESULT

These tests are carried out at the Jahad Daneshgahi high-pressure university lab (JDEVS) for the purpose of the assumptions discussed in this paper, as shown in Fig 14.

The cable used in this case is 2 meters with the specification Ducab power plus bico electric cable iec 60502-2 made in UAE 2005. To prove our assumptions, we performed these experiments at several voltages and recorded the results. In different

voltage cycles, there were various types of disturbances that we succeeded in recording the data accurately after re-calibrating the system.

Partial discharge tests can be classified into two categories:

- 1- Portable Checking and Tracing (OLPD)
- 2- Multi-channel diagnosis and troubleshooting

For portable testing and troubleshooting, testing equipment should be portable. We used wireless devices and conserve battery source in order to SETUP time and eliminate the risk of damage to cables and other necessary equipment. Troubleshooting equipment should be able to switch quickly between VHF, HFCT, and TEV ... in order to fully examine the high-pressure equipment, which is essential.

Cable joints and terminals are usually the most vulnerable devices to the occurrence of partial discharge and associated errors. Many defects are caused by human errors in the

process of installing insulation equipment. Fortunately, it is possible to detect quickly and track the insulation imperfections in joints and terminals using the VHF sensor. Generally, the existence of a cavity in the terminals is the main cause of the defect, and the presence of free electrons in the insulation and the occurrence of surface PDs can also occur.

As shown in Fig. 15, in the absence of disturbing signals, partial acoustic signals can be easily detected. As noted in Fig. 16, it should be noted that partial discharge is difficult to detect with mechanical vibration or mechanical noise in the environment and you can easily see that the simulation results are close to the result of the test. Another point, when using an acoustic sensor, is that the signals in the half-cycle are negative, as shown in Fig. 17. The corona signals are discharged and differentiate with partial discharge signals. Fig 18 shows the phase-AE spectra of the diffusion site and the phase angle of the amplitude. The color of the point



*Fig. 14. Laboratory and test circuit.*

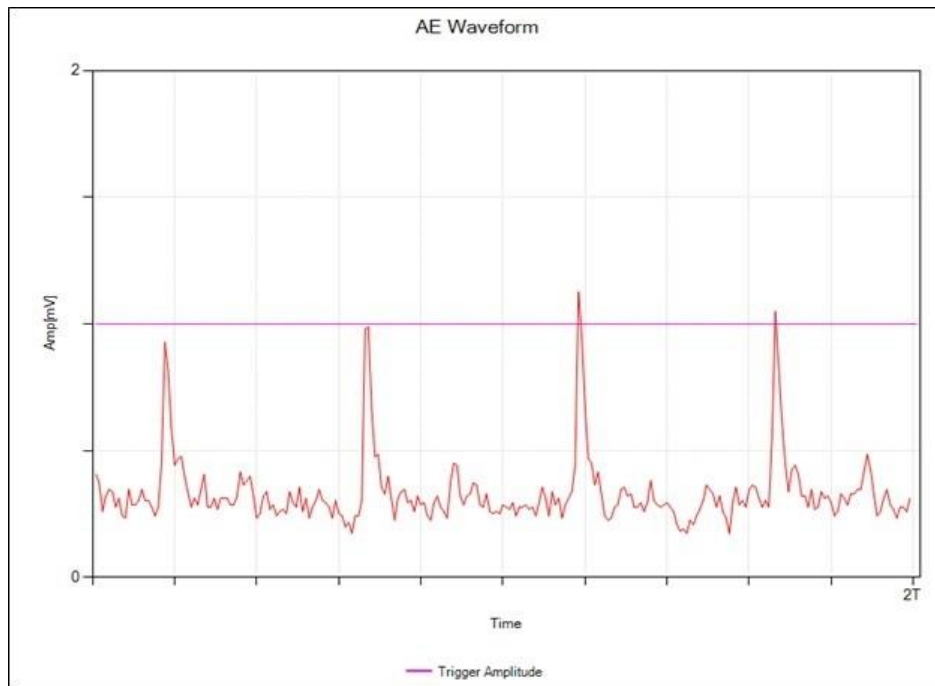


*Fig. 15. The waveform results from a partial discharge in cable.*

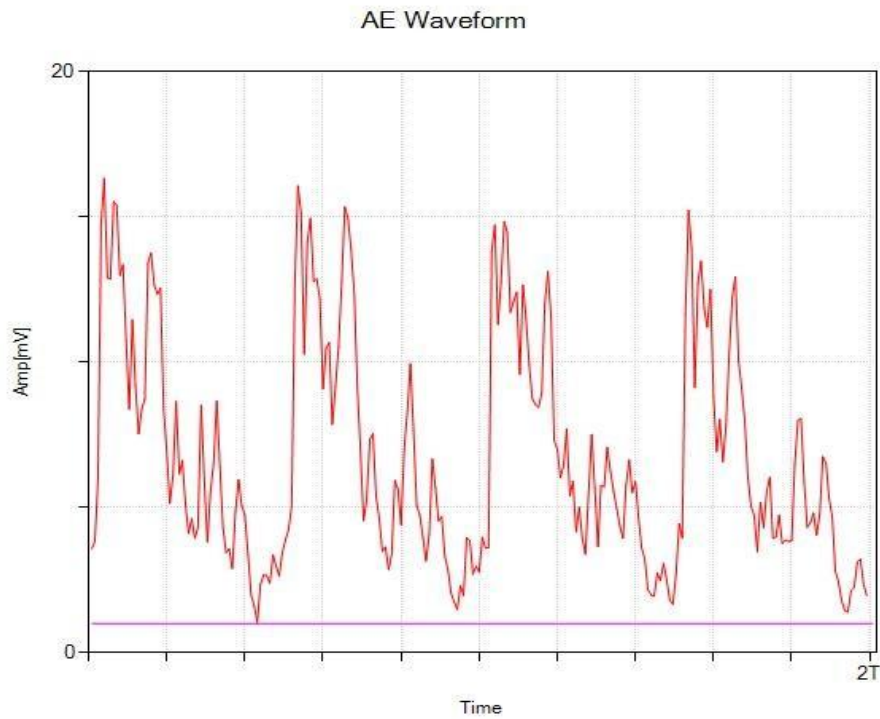


*Fig. 16. Acoustic waveform due to mechanical vibration.*

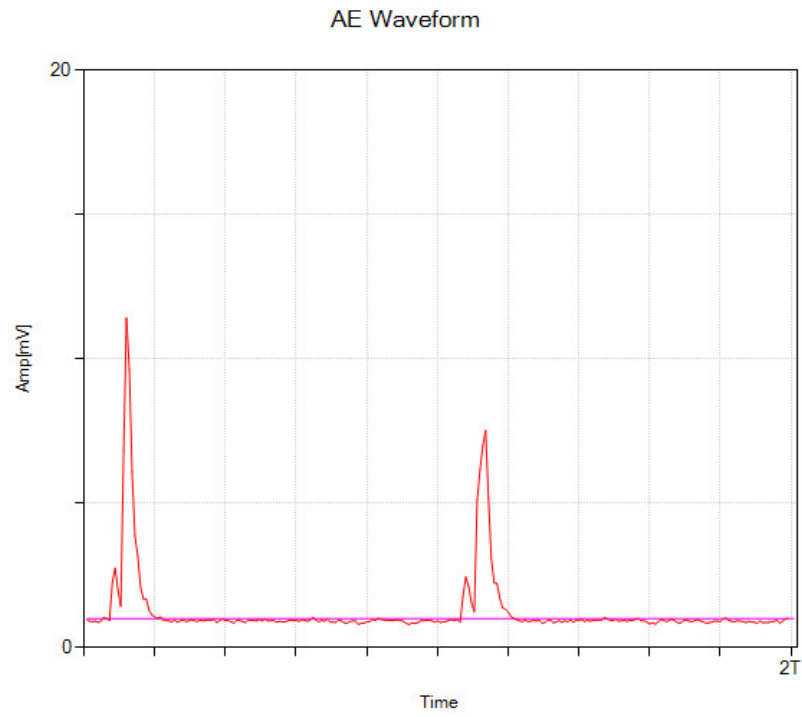
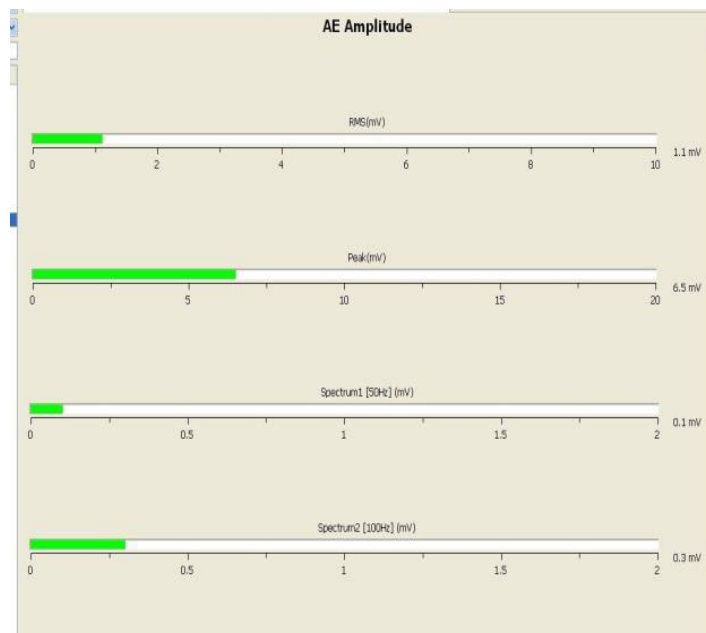
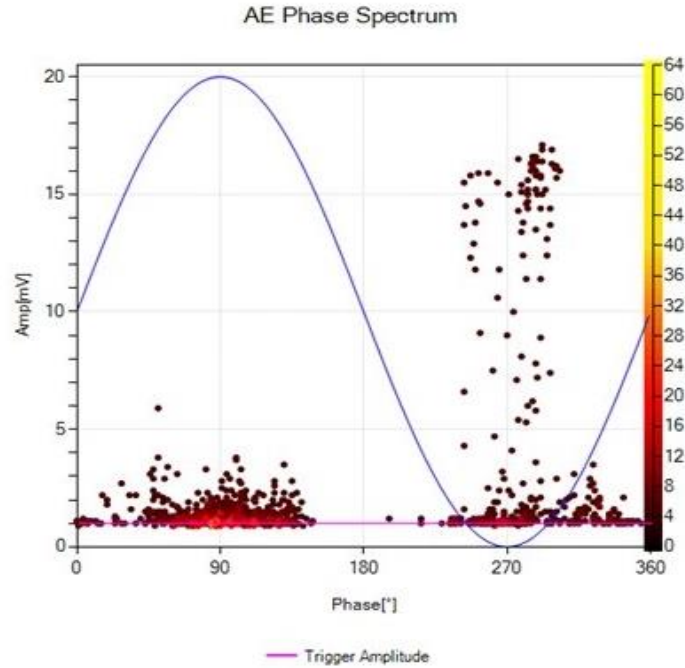


**Fig. 17. Corona wave diagram only in negative cycle.**



**(a)**

**Continued**



(b)

Fig. 18. (a) The AE Amplitude mode displays the RMS amplitude, peak amplitude, 60Hz resonance, and 120Hz resonance (b) AE Phase Spectrum of mechanical vibration.

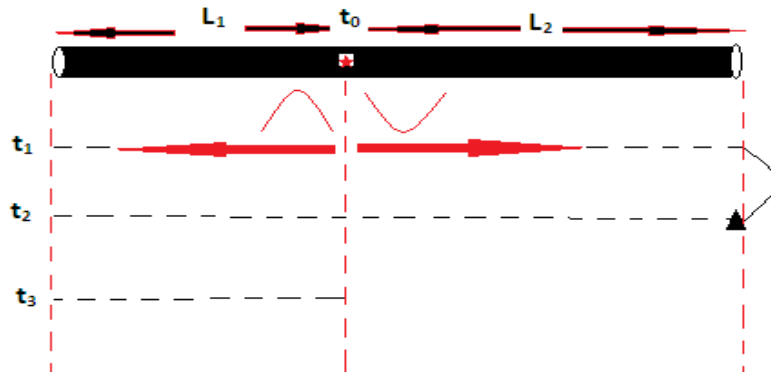


Fig. 19. Schematic view of acoustic waveforms.

represents the density of that signal type. The color will change from blue to red and then to yellow as multiple signals arrive with the same amplitude and phase timing. The fig, 18 shows the AE phase spectrum of a surface tracking PD activity. The pulses have various amplitudes. The pulses are different on the negative and positive half-cycles.

As you can see in Fig 19, the method of issuing and receiving acoustic waves due to the occurrence of partial discharge in the cavity whose effective parameters are expressed as follows.

$$L = L_1 + L_2 \quad (9)$$

$$V = \frac{1}{\sqrt{LC}} \quad (10)$$

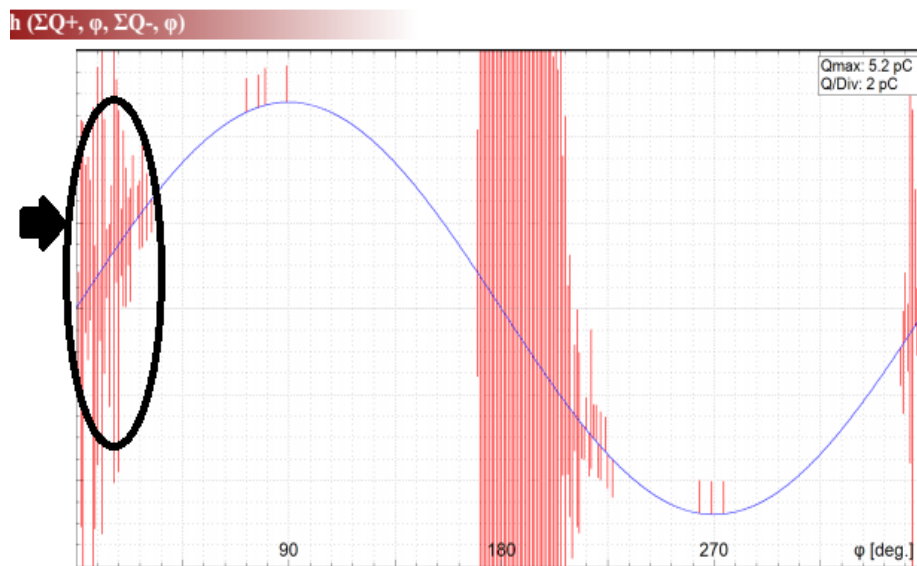
$$t_1 = \frac{L_2}{V} = \frac{L - L_1}{V} \quad (11)$$

$$t_2 = \frac{L_1 + L}{V} \quad (12)$$

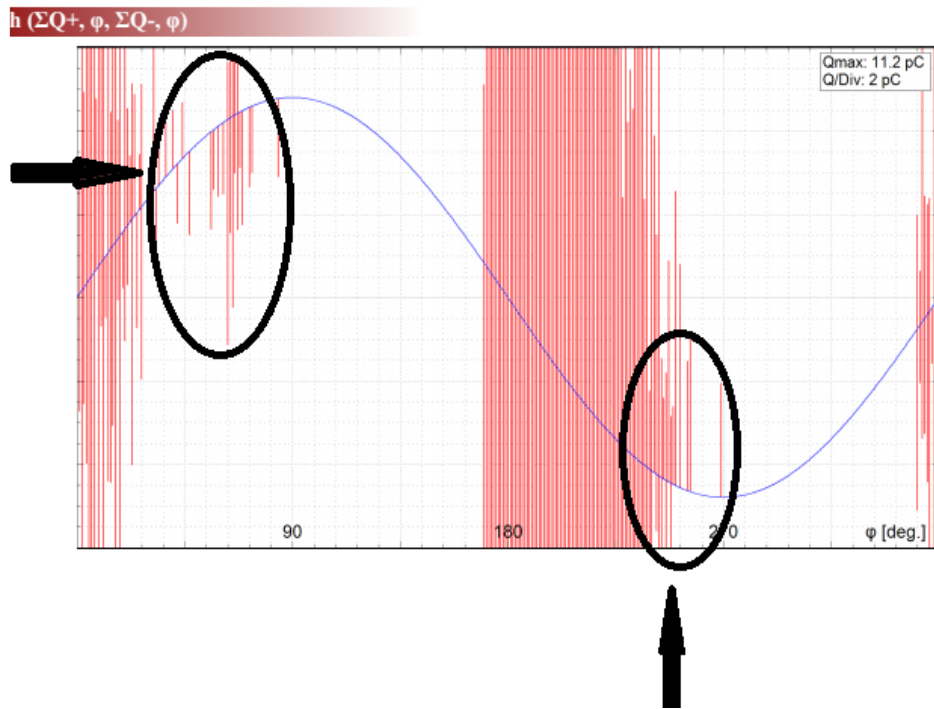
According to the results obtained from the experiments and having L and C values of the case, the discharge voltage can be calculated using the formula 10. Then we can easily determine the defect location, which is the same as  $L_1$  according to the time of arrival, the discharge voltage and the length of the cable. Because it is only unknown in  $L_1$  relations.

Cavernous drainage usually creates weak VHF waves that can be detected at less than 6 ft. If the terminals are inside the box, VHF signals can detect and troubleshoot input and output. VHF waves that are derived from the results of partial discharge tests indicate that this type of discharge usually occurs in a phase or multiphase.

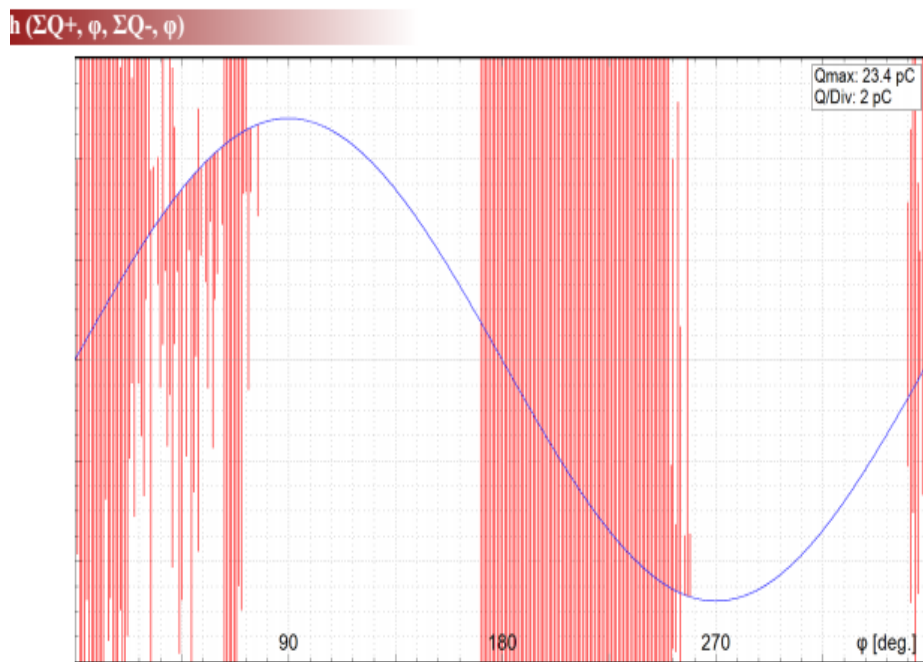
Usually, 80% of the partial discharge signals are very weak and unidentifiable, and from the remaining 20%, only a small number of signals are a real partial discharge signals which contain large amounts of environmental noise. Charges and evacuations revealed in the PCs range represent the number and number of free electrons. The distribution spectra of VHF and AE signals are monitored while the signals of different types of PDs are very similar. As you can see in the different sections of Fig. 20, the graphs summarize the positive and negative signals and the frequency of the occurrence of incomplete electrical discharges (whether the discharge is due to the presence of a cavity or partial discharge, and the corona discharge, etc.) in the different phases. Subsequent quantities, such as phase dependent functions, are usually used to describe the behaviour of feedback on PD activities. Partial discharging phase analyzer devices have PD detection



(a)  
Continued



(b)



(c)

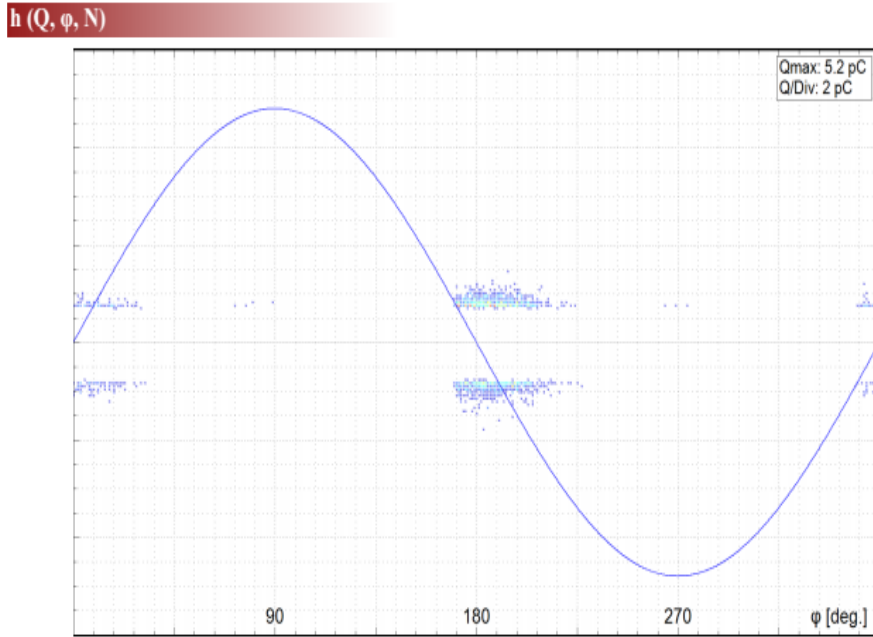
**Fig. 20. (a), (b) and (c) The partial discharge recorded by us in three steps corresponds to the voltage of 8.1 kV 17.3 kV and 20 kV respectively.**

functionality in the range of 0 to 360 degrees in a specific period of detection and predictive control. This will cause that we get

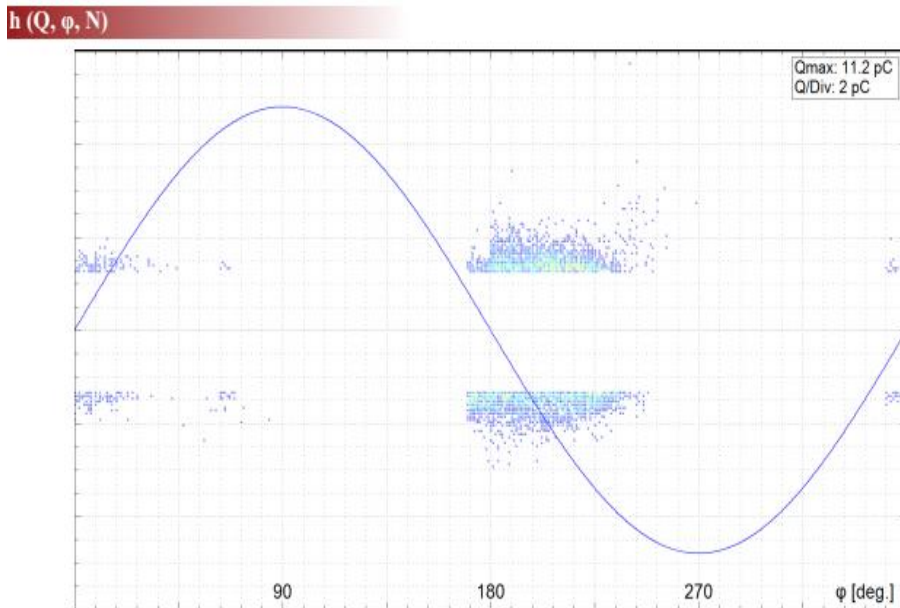
good information on the partial discharge in a cycle of voltage. This information includes the size of PD - Number of PDs - The average

size of PDs and the maximum amount of electrical discharges. VHF signals are very high and based on boosting power. Signals are widespread throughout the half-cycle width and visible in both the positive and

negative half-cycles. The results of the evaluation of VHF sensors for measurements indicate that surface depletion usually occurs

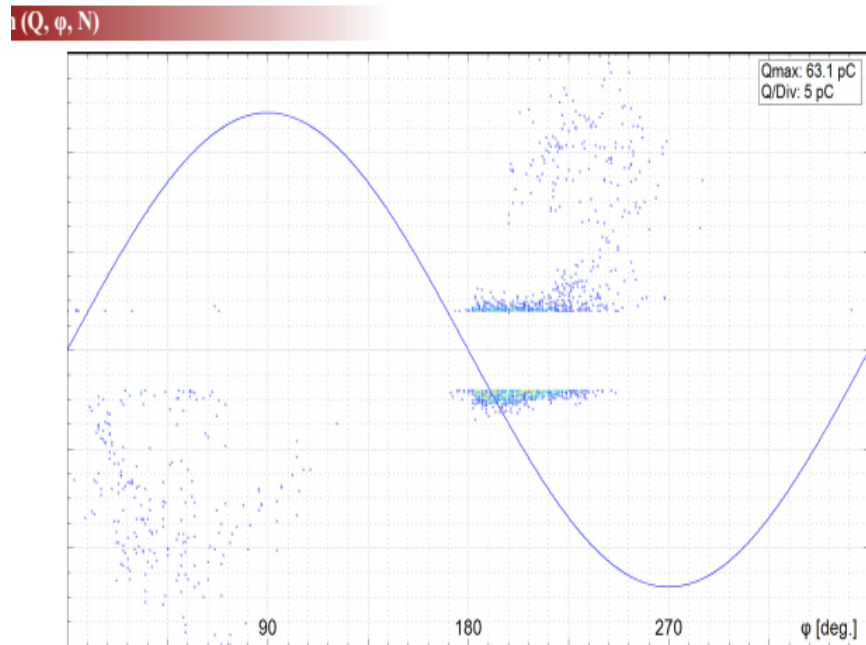


(a)



(b)

*Continued*



(c)

**Fig. 21. (a), (b) and (c) The partial discharge analyze of  $h(Q, \phi, N)$  by us in three steps corresponds to the voltage of 8.1 kV 17.3 kV and 20 kV respectively.**

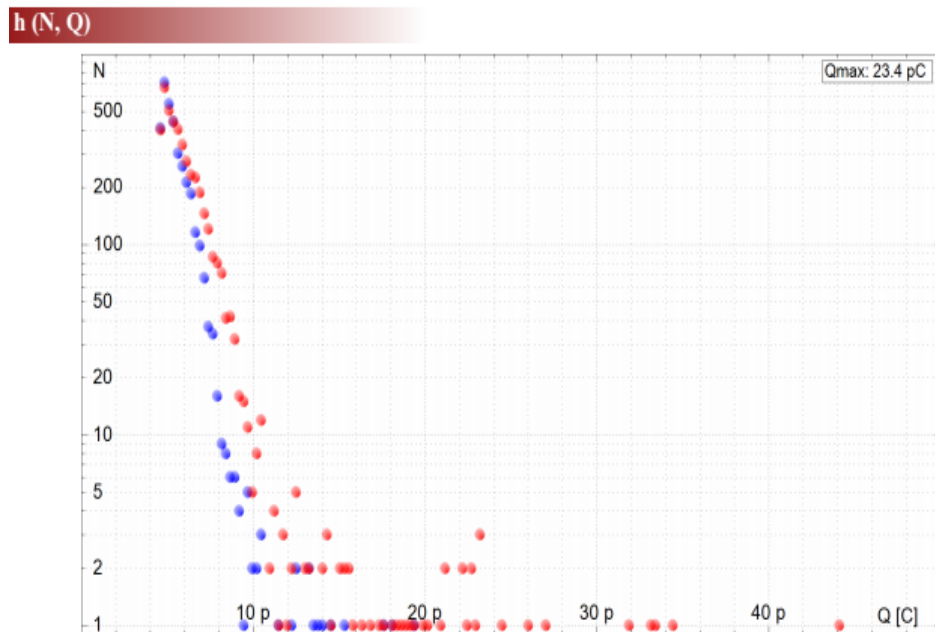


**Fig. 22. The number of partial discharges in 20kv test setup.**

in a half-cycle due to the massive movement of electrons from the ground to the conductor

(Fig. 20-a). The VHF signals from corona discharge have a small amount of amplitude,

and only in the half-cycle are negative as a result of the release of the electron from the conductor and the ionization of the surrounding area. The partial discharge signals on the effect of the cavity are also well-marked in the figure (Fig. 20-b). It might be difficult in some cases to detect this type of discharges (Fig. 20-c). Also, in fig. 21 you can see the accumulation on all kind of electrical discharge in different phases and voltages from different stages of the test. Fig. 22 also shows the number of PDs in distinct charges. Therefore, the acoustic chart can help to detect a partial discharge signal and locate it unilaterally or bilaterally. In this way, defective points can be manually determined by moving the AE sensor on the cable connections. Furthermore, the results of this study could be used as a reference point for troubleshooting partial discharges reliability in high cables.

#### 4. CONCLUSION

This paper describes the partial discharge error in XLPE cables by combining the results of two types of VHF and AE sensors for online troubleshooting. The following results can be deduced while the experimental results are also confirmed by simulation results. Online Troubleshooting, with the use of the VHF self-ignition sensor and its installation on the end of the earth's system, is easily achieved and can be used for analysis using the PRPDA (Phase Resolve PD analysis) method. For online surveys, partial discharge identification patterns are divided into the following three categories: Clear patterns, suspicious patterns, and discharge of no pattern. This method is capable of removing significant amounts of

disturbing signals and noise and capable of covering the frequency range from 1 to 100 MHz by the VHF sensor. The sensitivity of the online and on-site troubleshooting methods of the partial discharge, using a VHF sensor, is several PCs to several thousand PCs. VHF troubleshooting is able to identify the types of defects caused by incomplete electrical drafts in the cable, including corona discharge, partial discharge, and floating discharge. To locate the location of the partial discharge, it is easy to identify the defect location using the acoustic sensor's results. The combination of two VHF and AE sensors for troubleshooting can widely prevent electrical and electromagnetic interference.

#### REFERENCES

- [1] Barry H. Ward, A survey of new techniques in insulation monitoring of power transformers [J], IEEE Electrical Insulation Magazine, 2001, pp: 16-23;
- [2] Crichton G.C., Karlsson P. W. & Pedersen A., "Partial discharges in ellipsoidal and spheroidal voids", IEEE Trans. Electrical Insulation, pp: 335-342, 1989.
- [3] Gabe P.E. & Alex G. "Partial discharge theory and technologies related to medium voltage electrical equipment", Institute of Electrical And Electronic Engineers IAS 34 th Annual Meeting, 2000
- [4] H.-D. Schlemper, K. Feser, H.Blaum, P.Kirchesch, Sensitivity of Acoustic PD detection in GIS Laboratory experiments and on-site experience[C]. Conference Record of the 1996 IEEE

- International Symposium on Electrical Insulation, Montreal, Quebec, Canada, June 16-19, 1996, pp: 99-102;
- [5] Danikas M.G., George E. V., "The case of Pedersen's theory to model partial discharges in cavities enclosed in solid insulation: a criticism of some of its aspects from an electrical engineer's and from a physicists' point of view' *Journal of electrical engineering* , 2001, pp: 166-170.
- [6] Y Tian, P L Lewin, A E Davies, G Hathaway, *Acoustic Emission Techniques for partial discharge detection within cable*[C]. *Dielectric Materials, Measurements and applications Conference Publication No. 473, IEE 2000*, pp: 503-508;
- [7] Edin H., *Partial Discharges Studied with Variable Frequency of the Applied Voltage*. Sept 14, Stockholm, Sweden: Kungl Tekniska Högskolan, TRITAEEK-0102., 2001.
- [8] Wei Wang, Bin Wei, Chengrong Li, Lijian Ding, Changyu Li, Dong Liu." *VHF PD Detection of 110kV XLPE Cable Accessories*". *Conference Record of the 2004 IEE International Symposium on Electrical Insulation, Indianapolis, IN USA, 19-22 September 2004*.
- [9] Xin Li, Chengrong Li, Wei Wang, Bin Wei, Weijiang Wan." *Partial Discharge Measurement in XLPE Cable Joint by Using VHF Sensor*". *2004 International Conference on Solid Dielectrics, Toulouse, France, July 5-9, 2004*.
- [10] S. Meijer', R.A. Jongen', E. Gulski', P.P. Seitz, T.J.W.H. Hermans and L. Lamballais . "VHF Partial Discharge Detection during After-Laying testing of Power Cables ". *2007 International Conference on Solid Dielectrics, Winchester, UK, July 8-13, 2007*.
- [11] Y. Tian, P. L. Lewin, A. E. Davies., "Partial Discharge Detection in Cables Using VHF Capacitive Couplers " . *IEEE Transactions on Dielectrics and Electrical Insulation* . April 2003
- [12] CIGRE WG 21-05, "Partial Discharge Detection by Means of Acoustic Detection", 1993.
- [13] M. Ekherg, A. Gustafsson, M. Leijon, T. Bengtsson, T. Eriksson, C. Tomkvist, K. Iohansson, and L. Ming, "Recent Results in HV Measurement Techniques", *IEEE Trans. DEI, Vol. 2*, pp: 9n6-911 1995.
- [14] L. E. Lundgaard and W. Hansen, "Acoustic Method for Quality Control and In-Service Periodic Monitoring of Medium Voltage Cable Terminations", *International Symposium on Electrical Insulation (SEI), Virginia, USA*, and pp: 130-133, 1998.
- [15] Y. Tian, P. L. Lewin, A. E. Davies, and G. Hathaway, "Acoustic Emission Techniques for Partial Discharge Detection within Cable Insulation". *Proc. of 8th International Conference on Dielectric Materials, Measurements and Applications (DI (VIMA))*, pp: 503-508, Edinburgh, UK, 2000.
- [16] Wei Wang , Xu Cheng , Chong Liu , Fei Zong , Xueliang Shen ., "Detection Method of Partial Discharge in XLPE Cable Accessories Based on the Method of VHF Combined with Acoustic Emission ". *Proceedings of 2008 International Symposium on*

- Electrical Insulating Materials, September 7-11, 2008, Yokkaichi, Mie, Japan .
- [17] Zhao, X.L., Asada, T., Odendaal, W.G. and Van Wyk, J.D. (2003) an Overview of Integratable Current Sensor Technologies. Industry Applications Conference, 38th IAS Annual Meeting, 2, 1251-1258.
- [18] Robles, G., Argueso, M., Sanz, J., Giannetti, R. and Tellini, B. (2007) Identification of Parameters in a Rogowski Coil Used for the Measurement of Partial Discharges. IEEE Instrumentation and Measurement Technology Conference (IMTC) Proceedings, Warsaw, 1-3 May 2007, 1-4.
- [19] Jalebi, A. and McMahan, R. (2007) High-Performance Low-Cost Rogowski Transducers and Accompanying Circuitry. IEEE Transactions on Instrumentation and Measurement, 3, pp: 354-358.
- [20] Poncelas, O., Rosero, J.A., Cusido, J., Ortega, J.A. and Romeral, L. (2008) Design and Application of Rogowski Coil Current Sensor without Integrator for Fault Detection in Induction Motors. IEEE International Symposium on Industrial Electronics, Cambridge, 30 June-2 July 2008, pp: 558-563.
- [21] Zhu, J., Yang, L., Jia, J. and Zhang, Q. (2005) the Design of Rogowski Coil with Wide Band Using for Partial Discharge Measurements. Proceeding of International Symposium on Electrical Insulating Materials, 5-9 June 2005, pp: 518-521.
- [22] Z.D. Wang, P.A. Crossley and K.J. Comick, "A Simulation Model for Propagation of Partial Discharge Pulses in Transformers" IEEE 1998 pp: 151-155.
- [23] Shi Chen and Tadeusz Czaszejko, "Partial discharge test circuit as a spark gap transmitter" IEEE Electrical Insulation Magazine May/June 2011- Vol. 27, No. 3
- [24] Gavita Mugala, Roland Eriksson, "Dependence of XLPE Insulated Power Cable Wave Propagation Characteristics on Design Parameters", IEEE Transactions on Dielectrics and Electrical Insulation Vol. 14, No. 2; April 2007